DOI: 10.1021/ic101542m

Inorganic Chemistry
Article

Nature of Transannular Intramolecular Interactions in Group 4 and 6 Metallatranes: A Combined Density Functional Theory and Atoms in Molecules Theory Study

Ashwini K. Phukan* and Ankur Kanti Guha

Department of Chemical Sciences, Tezpur University, Napaam 784028, Assam, India

Received May 4, 2010

Density functional calculations coupled with quantum theory of atoms in molecules analysis were carried out on Group 4 and 6 metallatranes with special emphasis on the nature of transannular M···N bonds present in these molecules. Substituents at both the apical and equatorial positions are found to influence the extent of transannular interaction. The degree of pyramidalization around the metal and the bridgehead nitrogen atom play a key role in strengthening or weakening the M···N bond. The stability of these molecules are found to depend to a large extent on the strength of M···N bonds with significant contribution coming in from metal-equatorial and metal-apical bonds. Group 6 metallatranes are found to have stronger transannular bonds and, hence, higher stabilization energies than their Group 4 counterparts. Atoms in molecules theory analysis reveals the presence of a considerable amount of covalent character in the M···N bonds which increase from Group 4 to Group 6.

1. Introduction

Tripodal ligands such as triamidoamine $[(RNCH_2CH_2)_3N]^{3-}$ ($R = SiR'_3$, R' = aryl, alkyl), triethanolatoamine $[(OCH_2CH_2)_3N]^{3-}$, and its sulfur analogs have attracted considerable interest over a period of time.[1] They bind to main group and transition metals in a tetradentate manner to create a sterically protected, 3-fold-symmetric pocket around the metal atom[1a,d] having either a trigonal monopyramidal or bipyramidal geometry. The molecules so formed are popularly known as metallatranes featuring a transannular M···N bond. These metallatranes are widely used as catalysts for olefin polymerization and organometallic chemical vapor deposition (OMCVD) of thin films.[2] Among the transition metal atranes, those formed by Group 4 and Group 6 elements are extensively reported in the literature,[2−8] and the researchers found widespread use in various catalytic processes.[2,3,9−12]

The chemistry of these metallatranes are largely governed by the extent of transannular M···N interaction as well as the nature of substituents at the equatorial (E) and apical (Z) positions. The experimentally characterized metallatranes show a varying degree of M···N interaction (Table 1). However, these transannular distances are much shorter than the sum of the van der Waals radii of the respective metal and the bridgehead nitrogen atom. Large numbers of metallatranes involving both main group metals[13] as well as transition

*To whom correspondence should be addressed. Phone: +91 (3712) 267173. Fax: +91 (3712) 267005. E-mail: ashwini@tezu.ernet.in.

(1) (a) Verkade, J. G. *Coord. Chem. Rev*. **1994**, *137*, 233–295. (b) Chuit, C.; Corriu, R. J. P.; Reyé, C.; Young, J. C. *Chem. Rev*. **1993**, *93*, 1371–1448. (c) Pestunovich, V.; Kirpichenko, S.; Voronkov, M. In *The Chemistry of Organic Silicon Compounds*; Rappoport, Z., Apeloig, Y., Eds.; John Wiley & Sons: New York, 1998; Vol. *2*, Part 1, Chapter 24. (d) Schrock, R. R. *Acc. Chem. Res*. **1997**, *30*, 9–16.

(2) (a) Duan, Z.; Verkade, J. G. *Inorg. Chem*. **1995**, *34*, 4311–4316. (b) MacMillan, S. N.; Tanski, J. M.; Waterman, R. *Chem. Commun*. **2007**, 4172–4174. (c) Kim, Y.; Hong, E.; Lee, M. H.; Kim, J.; Han, Y.; Do, Y. *Organometallics* **1999**, *18*, 36–39.

(3) (a) Zanetti, N. C.; Schrock, R. R.; Davis, W. M. *Angew. Chem., Int. Ed. Engl*. **1995**, *34*, 2044–2046. (b) Scheer, M.; Muller, J.; Haser, M. *Angew. Chem., Int. Ed. Engl*. **1996**, *35*, 2492–2496.

(4) (a) Schubart, M.; O'Dwyer, L.; Gade, L. H.; Li, W. S.; Mcpartlin, M. *Inorg. Chem*. **1994**, *33*, 3893–3898. (b) Duan, Z.; Naiini, A. A.; Lee, J. H.; Verkade, J. G. *Inorg. Chem*. **1995**, *34*, 5477–5482.

(5) (a) Morton, C.; Munslow, I. J.; Sanders, C. J.; Alcock, N. W.; Scott, P. *Organometallics* **1999**, *18*, 4608–4613. (b) Morton, C.; Gillespie, K. M.; Sanders, C. J.; Scott, P. *J. Organomet. Chem*. **2000**, *606*, 141–146.

(6) (a) Smythe, N. C.; Schrock, R. R.; Muller, P.; Weare, W. W. *Inorg. Chem*. **2006**, *45*, 7111–7118. (b) Filippou, A. C.; Schneider, S. *Organometallics* **2003**, *22*, 3010–3012. (c) Filippou, A. C.; Schneider, S.; Ziemer, B. *Eur. J. Inorg. Chem*. **2002**, 2928–2935.

(7) Schrock, R. R.; Seidel, S. W.; Zanetti, N. C.; Shih, K. Y.; O'Donoghue, M. B.; Davis, W. M.; Reiff, W. M. *J. Am. Chem. Soc*. **1997**, *119*, 11876–11893.

(8) (a) Scheer, M.; Muller, J.; Baum, G.; Haser, M. *Chem. Commun*. **1998**, 2505–2506. (b) Schrock, R. R.; Seidel, S. M.; Zanetti, N. C.; Dobbs, D. A.; Shih, K. Y.; Davies, W. M. *Organometallics* **1997**, *16*, 5195–5208. (c) Seidel, S. W.; Schrock, R. R.; Davies, W. M. *Organometallics* **1998**, *17*, 1058–1068.

(9) (a) Hirose, M.; Yasui, T.; Ochi, Y.; Nakagawa, M. U. S. Patent, 4, 420, 498, 1983. (b) Buhl, R.; Pulker, H. K.; Moll, E. *Thin Solid Films* **1981**, *80*, 265–270.

(10) (a) Ajjou, J. A. N.; Scott, S. L.; Paquet, V. *J. Am. Chem. Soc*. **1998**, *120*, 415–416. (b) Ajjou, J. A. N.; Rice, G. L.; Scott, S. L. *J. Am. Chem. Soc*. **1998**, *120*, 13436–13443. (c) Monoi, T.; Ikeda, H.; Torigoe, H. Eur. Patent 1041085, 2000. (d) Ajjou, J. A. N.; Scott, S. L. *J. Am. Chem. Soc*. **2000**, *122*, 8968–8976. (e) Schmid, R.; Ziegler, T. *Can. J. Chem*. **2000**, *78*, 265–269. (f) Scott, S. L.; Ajjou, J. A. N. *Chem. Eng. Sci*. **2001**, *56*, 4155–4168.

(11) Schmid, R.; Ziegler, T. *Organometallics* **2000**, *19*, 2756–2765.

(12) (a) Kol, M.; Schrock, R. R.; Kempe, R.; Davis, W. M. *J. Am. Chem. Soc*. **1994**, *116*, 4382–4390. (b) O'Donoghue, M. B.; Zanetti, N. C.; Davis, W. M.; Schrock, R. R. *J. Am. Chem. Soc*. **1997**, *119*, 2753–2754.

(13) (a) Pinkas, J.; Gaul, B.; Verkade, J. G. *J. Am. Chem. Soc*. **1993**, *115*, 3925–3931. (b) Pinkas, J.; Wang, T.; Jacobson, R. A.; Verkade, J. G. *Inorg. Chem*. **1994**, *33*, 5244–5253. (c) Shutov, P. L.; Karlov, S. S.; Harms, K.; Tyurin, D. A.; Churakov, A. V.; Lorberth, J.; Zaitseva, G. S. *Inorg. Chem*. **2002**, *41*, 6147–6152. (d) Kim, Y.; Verkade, J. G. *Inorg. Chem*. **2003**, *42*, 4804–4806.

Published on Web 09/30/2010

Table 1. List of Experimentally Known Structures of Group 4 and 6 Metallatranes (Z-M[-ER(CH_2)$_2$-]$_3$N) for Which Crystal Structures Are Available[a,b]

metal	E	Z	ranges of $r_{M\text{-}Nax}$ (Å)	references
Ti	NR, O	Cl, NR'_2, OR′, OAr[c]	2.006−2.451	2, 4
Zr	NR	Cl, NR'_2, CH_3, PHPh, CH_2Ph	2.393−2.548	2b, 5
Hf	$NSi(CH_3)_3$	$N(CH_3)_2$	2.488	4b
Cr	NR, NAr[d]	H, F, Cl, Br, CN, NO, CO, CH_3	2.043−2.288	6
Mo	NR, NAr[e], NAr[d], S	Cl, NH_3, NNR′, NR′, N_2, C_2H_5,CD_3, cyclo-C_6H_{11}, CN, PHPh, OR′, NO	2.171−2.422	3a, 7
W	NR, NAr[d]	Cl, N_2, NNR, cyclo-C_4H_7, CO, OR′	2.174−2.395	3b, 8

[a] Here, E is the equatorial substituent and Z is the apical ligand. [b] R = H, CH_3, C_2H_5, i-Pr, $CH_2(^tBu)$, C_6F_5, $Si(CH_3)_3$, $(CH_3)_3C_6H_2$, $(^tBu)_2C_6H_3$, $(CF_3)_2C_6H_3$, $Si(CH_3)_2(^tBu)$. R′ = CH_3, SO_2CF_3, $(^tBu)_2C_6H_3$, $(CH_2Ph)(CHPPh)$, $(CH_3)_2C_6H_3$, $Si(CH_3)_3$, $SiPh_3$, $Si(i\text{-}Pr)_3$. [c] Ar = $(^tBu)_2C_6H_2CPh_2$, $(^tBu)_2C_6H_2C(Ph)(^tBu)_2OHC_6H_2$, $(iPr)_2C_6H_3$. [d] Ar = $(i\text{-}Pr_3C_6H_2)_2C_6H_3$. [e] Ar = $(^tBu_3C_6H_2)_2C_6H_3$.

Scheme 1

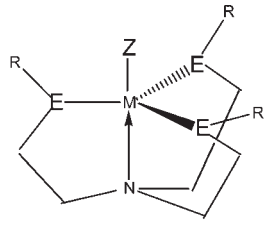

M = Ti, Zr, Hf, Cr, Mo, W ; E = NR, O, S ; R = H, CH_3, SiH_3

Z = Cl, NH_2, CO, CN, NH_3, CH_3, OH, H_2O

metals (Table 1) are reported to date. While the literature is enriched with theoretical studies of main group atranes,[14] such studies related to transition metal atranes are very few.[15] Gordon and co-workers have carried out ab initio calculations on the molecular structure of a series of azatitanatranes. Their studies reveal that the transannular Ti···N interaction is stronger than those found for analogous azasilatranes.[15a] Filippou's group has reported the first structurally characterized trigonal monopyramidal chromium(II) complexes with triamidoamine ligands and rationalized the structural changes theoretically.[15b] Thus, it is worthwhile to carry out a systematic study on the structural trends of these metallatranes. We present here a comprehensive study on the effect of substituents at the metal and equatorial atom on the structure and stability of Group 4 and 6 metallatranes. A variety of substituents were employed at the metal so that the effect of both σ-donor as well as π-donor/acceptor ligands can be studied (Scheme 1). Also, the range of substituents is considerably larger than that of experimentally known compounds. Our main emphasis will be on the nature of transannular M···N interaction as a function of E and Z. Besides this transannular M···N interaction, any other factors which may enhance the stability of these molecules are also explored. In all our discussions, we will use the prefixes aza, azamethyl, azasilyl, oxa, and thia to indicate metallatranes with NH, NCH_3, $NSiH_3$, O, and S as the equatorial substituents. All the metallatrane molecules considered in this study are neutral.

(14) (a) Windus, T. L.; Schmidt, M. W.; Gordon, M. S. *J. Am. Chem. Soc.* **1994**, *116*, 11449–11455. (b) Schmidt, M. W.; Windus, T. L.; Gordon, M. S. *J. Am. Chem. Soc.* **1995**, *117*, 7480–7486. (c) Korlyukov, A. A.; Lyssenko, K. A.; Antipin, M. Y.; Kirin, V. N.; Chernyshev, E. A.; Knyazev, S. P. *Inorg. Chem.* **2002**, *41*, 5043–5051. (d) Soran, A. P.; Silvestru, C.; Breunig, H. J.; Balázs, G.; Green, J. C. *Organometallics* **2007**, *26*, 1196–1203.

(15) (a) Rioux, F.; Schmidt, M. W.; Gordon, M. S. *Organometallics* **1997**, *16*, 158–162. (b) Filippou, A. C.; Schneider, S.; Schnakenburg, G. *Inorg. Chem.* **2003**, *42*, 6974–6976.

2. Computational Details

All the structures were fully optimized with gradient-corrected density functional theory (DFT) using the Becke's three-parameter hybrid functional (B3LYP) with exchange correlation functional of Lee, Yang, and Parr.[16] We employed the LANL2DZ basis set with the effective core potentials (ECP) of Hay and Wadt.[17] All the structures were verified as a minimum by confirming that their respective Hessian (matrix of analytically determined second order energy derivative) is all real. The bonding nature of all the compounds were analyzed by natural bond orbital analysis (NBO).[18] All the computations were performed using the Gaussian 03 suite program.[19] The oxidation states and, thus, the d-electron count at the central metal atom changes with variation in the nature of apical ligands (Z). For neutral Z groups, the d-electron count at the metal atom is 1 and 3 for the Group 4 and 6 metals, respectively, whereas for anionic Z groups, the d-electron count decreases by one unit to 0 and 2, respectively. For the Group 6 metals in +3 oxidation state, both the spin states (high and low) were considered. In order to understand the nature of bonding in these molecules in greater detail, the topological properties of the resultant electron density, ρ, obtained from the wave functions of all the optimized structures were analyzed with the quantum theory of atoms in molecules (QTAIM).[20] The QTAIM analysis were carried out with the programs AIMPAC[21] and AIMALL[22] whereas the wave functions were generated with Gaussian 03 at the same level of theory as was used for geometry optimization.[19] However, to produce the contour plots of the laplacian with AIMALL, the corresponding wave functions were generated by running single point calculations at B3LYP/6-31+G* level of theory.

3. Results and Discussion

3.1. Molecular Geometry. The molecular structure of metallatranes consists of three five membered envelope shaped rings with the transannular M···N bond being

(16) B3LYP is Becke's three-parameter hybrid method using the LYP correlation functional. (a) Becke, A. D. *J. Chem. Phys.* **1993**, *98*, 5648–5652. (b) Lee, C.; Yang, W.; Parr, R. G. *Phys. Rev. B* **1988**, *37*, 785–789. (c) Vosko, S. H.; Wilk, L.; Nusair, M. *Can. J. Phys.* **1980**, *58*, 1200–1211.

(17) (a) Hay, P. J.; Wadt, W. R. *J. Chem. Phys.* **1985**, *82*, 270–283. (b) Wadt, W. R.; Hay, P. J. *J. Chem. Phys.* **1985**, *82*, 284–298. (c) Hay, P. J.; Wadt., W. R. *J. Chem. Phys.* **1985**, *82*, 299–310.

(18) (a) Glendening, E. D.; Reed, A. E.; Carpenter, J. E.; Weinhold, F. *NBO Program 3.1*: University of Wisconsin: Madison, W. T., 1988. (b) Reed, A. E.; Weinhold, F.; Curtiss, L. A. *Chem. Rev.* **1988**, *88*, 899–926.

(19) Frisch, M. C. et al. *Gaussian 03*, revision D.02; Gaussian, Inc.: Wallingford CT, 2004. For complete reference, see Supporting Information 2004.

(20) (a) Bader, R. F. W. *Atoms in Molecules: a Quantum Theory*; Oxford University Press: Oxford, U. K., 1990. (b) Bader, R. F. W. *J. Phys. Chem. A* **1998**, *102*, 7314–7323. (c) Bader, R. F. W. *Chem. Rev.* **1991**, *91*, 893–928.

(21) Bader, R. F. W. AIMPAC; http://www.chemistry.mcmaster.ca/aimpac/.

(22) Keith, T. A.; AIMAll (Version 10.02.09), 2010 (http://aim.tkgristmill.com).

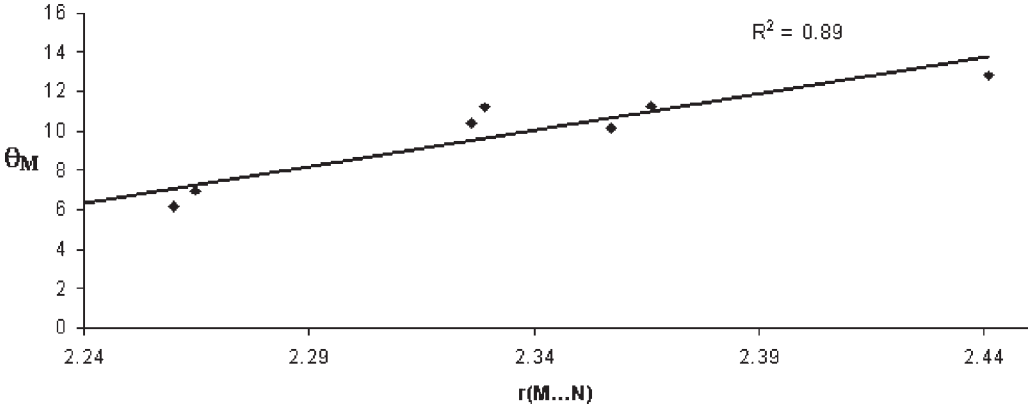

Figure 1. Variation of transannular Ti···N distance with pyramidalization at M (θ_M) for M = Ti and E = $NSiH_3$.

common to all the rings. The optimized geometries of these molecules adopt pseudotrigonal bipyramidal geometry around the metal atom (Figure S1, Supporting Information) with the metal and the bridgehead nitrogen atoms being pyramidalized outwardly and inwardly, respectively.

3.1.1. Group 4 Metallatranes. Comparison of the X-ray bond lengths of titanatranes with our computed ones reveal that there is a close agreement between experiment and theory (Table S1, Supporting Information).[4a] On an average, the calculated transannular Ti···N distances are found to be 12.4% longer than the sum of the covalent radii (2.07 Å) for Ti and N. Similar results were obtained by the group of Gordon for azatitanatranes.[15a] Irrespective of the nature of the substituents at the equatorial position, the shortest transannular bonds are computed for the σ-donating apical ligands, viz., CO, NH_3, and H_2O. This can be explained by looking at the values of the pyramidalization angle at the metal (θ_M) and bridgehead nitrogen atom (θ_N; Table S1, Supporting Information). While θ_N do not vary appreciably with the changes either in the apical or in the equatorial substituents, θ_M decreases for these σ-donating ligands. In general, a decrease in θ_M and increase in θ_N makes it ideal for a strong transannular interaction (Figure 1). Corresponding to the increase or decrease of Ti···N distance, the Ti−Z distances decrease or increase accordingly. This is also reflected in the WBI values of respective bonds (Table S1, Supporting Information). For example, in the case of Cl and OH as the apical substituents, the Ti···N distance of azasilyltitanatrane is more than that of azamethyltitanatrane even though the value of θ_M is more for the latter than the former. This lengthening of the Ti···N bond can be explained by the apparent strengthening of the Ti−Cl and Ti−O bonds. However, this correlation was not observed for CO as, in this case, back-donation from the filled metal orbital to the π^* orbital of CO results in strengthening of the Ti−CO bond. Azamethyl and azasilyl titanatranes compute a shorter Ti···N bond. This is because the bulky methyl and silyl group orbitals force the metal atom to move toward the equatorial plane defined by the three nitrogen atoms, thereby enhancing the transannular interaction. Out of all the apical and equatorial substituents, Z = CH_3 and E = O computes the longest Ti···N distance. Our results are in contrast to those reported by Gordon and co-workers for the parent azatitanatrane geometry by taking CH_3 and NH_2 as the apical substituents. They found a longer Ti···N bond for NH_2 than CH_3. This difference may arise from the noninclusion of electron correlation in their study. The Ti···N bonds of oxatitanatranes are much longer than others. Interestingly, replacement of the oxygen atom by the heavier sulfur atom dramatically changes the structure. It results in slight deformation of the cage structure even though the trigonal bipyramidal geometry around the metal atom is retained to a large extent. The bigger sulfur atom causes a decrease and increase in the value of θ_M and θ_N, respectively. These geometrical changes at the metal and bridgehead nitrogen atom result in enhancement of the transannular interaction. NBO analysis reveals that the occupancy of the lone pair at the bridgehead nitrogen atom increases or decreases with respect to a decrease or increase in Ti···N distance.

The computed minimum energy structures of zirconatranes and hafnatranes are also in very good agreement with experimentally observed ones (Tables S2 and S3, Supporting Information).[4b,5a] The geometrical variation observed for these two metallatranes are similar to those observed for titanatranes. However, the transannular M···N bonds are weaker for heavier Group 4 elements which is consistent with the decrease in hardness of the participating metals. The M−E bond strengths also follow the same notion.

One interesting structural variation of these Group 4 metallatranes is that, with Z = NH_3 and H_2O, these metallatranes do not maintain the local C_3 axis as revealed by the < Z−M···N angle which is much less than 180°. This structural variation is more pronounced with oxygen as the equatorial substituent.

3.1.2. Group 6 Metallatranes. The important geometrical parameters for chromatranes are found to be reasonably close to the experimentally observed ones (Table S4, Supporting Information).[6a−c] The average lengthening of the calculated transannular Cr···N distances are found to be only 5% of the sum of the covalent radii (2.03 Å) of Cr and N. Depending on the nature of the ligands (neutral or anionic) at the apical position, the metal atom of these metallatranes, viz., Cr, Mo, and W, can exist in either +3 or +4 oxidation states. The relative stability of a particular spin state can be explained by invoking the spectrochemical series. As expected, the

Table 2. Relative Stability of the Different Spin States of Group 6 Metallatranes at Their +3 Oxidation State Computed at the B3LYP/LANL2DZ Level of Theory

		NH		NCH_3		$NSiH_3$		O		S	
apical ligands (Z)	metal (M)	S = 1/2	S = 3/2	S = 1/2	S = 3/2	S = 1/2	S = 3/2	S = 1/2	S = 3/2	S = 1/2	S = 3/2
CO	Cr	0.0	15.1	0.0	14.6	0.0	6.3	0.0	2.8	0.0	−4.2
	Mo	0.0	34.6	0.0	35.6	0.0	34.5	0.0	24.0	0.0	25.2
	W	0.0	43.3	0.0	43.0	0.0	40.5	0.0	27.3	0.0	36.4
NH_3	Cr	6.7	0.0	5.6	0.0	10.8	0.0	9.6	0.0	20.0	0.0
	Mo	0.0	15.3	0.0	15.4	0.0	11.5	0.0	7.3	0.0	4.0
	W	0.0	15.5	0.0	19.4	0.0	17.1	0.0	8.6	0.0	12.6
H_2O	Cr	*a*		*a*		7.6	0.0	8.5	0.0	15.6	0.0
	Mo	0.0	17.7	0.0	17.4	0.0	14.5	0.0	8.9	0.0	5.0
	W	0.0	8.1	0.0	10.8	0.0	14.9	0.0	10.9	0.0	14.8

[a] Broken structure.

strong field ligand CO results in stabilization of the doublet state for all the chromatranes except thiachromatranes. For thiachromatranes, the quartet state is more favorable than the doublet state by 4.2 kcal/mol (Table 2). Even with oxygen at the equatorial position, the energy difference between these two spin states is not very large, implying that the spin state of this class of organometallic compounds can be tuned by putting suitable substituents at the apical and equatorial positions. In other words, the reactivity of these compounds can be tuned by changing the spin state as changes in spin states are found to have a dramatic effect on chemical reactivity.[23]

For the weak field ligands, NH_3 and H_2O, the high spin (quartet) is the most stable state. In general, shorter and longer Cr···N distances are computed for neutral and anionic ligands, respectively, which can be correlated to their relative trans directing ability. While the weakly trans directing ligands (Cl, NH_3, H_2O, etc.) strengthen the Cr···N bond, the stronger ones (CO, CN, CH_3) weaken this bond. For a given equatorial substituent, the longest Cr···N bonds are computed for CH_3 as the apical ligand which is in tune with experimental observation.[6b] On the other hand, longer Cr···N bonds are obtained when the highly electronegative oxygen atom occupies the equatorial position. Like Group 4 metallatranes, thia derivatives of Group 6 metallatranes show similar structural variation. Optimization of the ground state chromatrane molecule with Z = H_2O and E = NH and NCH_3 leads to cleavage of a Cr−N bond, resulting in a broken structure, and thus, these two molecules were excluded from further discussion.

The calculated transannular Mo···N and W···N distances are reasonably closer to the experimentally observed ones (Tables S5 and S6, Supporting Information)[7,3b,8c] On an average, the calculated transannular Mo···N and W···N distances are found to be 7% and 9% longer than the sum of the covalent radii (2.15 Å) of Mo and N and (2.05 Å) of W and N atom, respectively. Compared to chromatranes, a doublet spin state is more stable for molybdenatranes and tungstenatranes, especially with CO as the apical ligand (Table 2). This is due to the higher d-orbital splitting as we go down a group resulting in pairing of the electrons. In fact, all the doublet structures of molybdenatranes and tungstenatranes with neutral apical ligands are more stable than the quartet ones. Barring few exceptions, the geometric variations obtained for these molecules are more or less similar to those found for their chromium analogs. Due to the soft character of Mo and W, M−S bonds are consistently stronger than M−O bonds.

Comparison of the geometrical parameters for Group 4 and Group 6 metallatranes reveals that the pyramidalization angles around the metal atoms are quite less for Group 6 metallatranes than for Group 4 ones. Natural charges computed using NBO[18] routine reveal that there is a decrease in the positive and negative charge at the metal center and at the bridgehead nitrogen atom, respectively, while going from Group 4 to Group 6 metallatranes. All these factors results in strengthening of the transannular interaction in Group 6 metallatranes.

3.2. Stabilization Energies. In general, the stability of these metallatranes are largely governed by the degree of M···N interaction with significant contribution coming in from M−E and M−Z bonds. With few exceptions, the stabilization energy increases or decreases with a decrease or increase in M···N interactions, respectively. We have used two different sets of equations to compute the stabilization energies of these metallatranes: one for the azametallatranes (eq 1) and the other for their chalcogen analogs (eq 2).

$$Z\text{−}M[(CH_2CH_2E)_3N] + 3NH_3 + 3CH_4 \rightarrow (CH_3CH_2)_3N + 3CH_3NH_2 + Z\text{−}M(NHR)_3 \qquad E = NR \qquad R = H, CH_3, SiH_3 \tag{1}$$

$$Z\text{−}M[(CH_2CH_2E)_3N] + 3H_2E + 3CH_4 \rightarrow (CH_3CH_2)_3N + 3CH_3EH + Z\text{−}M(EH)_3 \qquad E = O, S \tag{2}$$

The stabilization energies of Group 4 metallatranes increase with changes in equatorial substituents from NH to NCH_3 but decrease with $NSiH_3$ (Table 3) which can be correlated to an increase or decrease in transannular distances. However, there are exceptions.

For example, with CO as the apical ligand, stability of azamethyl titanatrane is higher than its silyl derivative even though the Ti···N distance of the former is longer than that of the latter. This can be explained by looking at the relative strengths of the respective Ti−Z and Ti−E bonds of these two molecules. Thiametallatranes are much more stable than oxa ones not only due to strong transannular interaction but also due to stronger M−E

(23) (a) Macedo, J. L. C.; Harvey, J. N. *J. Am. Chem. Soc.* **2004**, *126*, 5789–5797. (b) Poli, R. *J. Organomet. Chem.* **2004**, *689*, 4291–4304. (c) Wasbotten, I. H.; Ghosh, A. *Inorg. Chem.* **2007**, *46*, 7890–7898.

Table 3. B3LYP/LANL2DZ Computed Stabilization Energies for Group 4 and 6 Metallatranes[a]

Z	E = NH		NCH_3		$NSiH_3$		O		S	
	group 4	group 6	group 4	group 6	group 4	group 6	group 4	group 6	group 4	group 6
Cl	**21.6**	**66.1**	**27.6**	**62.3**	**16.6**	**61.3**	**15.8**	**66.7**	**27.5**	**67.8**
	22.4	37.9	33.2	47.8	17.9	35.6	12.2	30.2	27.9	38.2
	22.5	*53.6*	*34.1*	*47.5*	*19.2*	*40.0*	*9.5*	*43.9*	*29.8*	*48.6*
NH_2	**19.1**	**46.9**	**23.3**	**46.7**	**16.1**	**45.7**	**14.5**	**53.1**	**24.4**	**51.9**
	19.4	31.0	31.8	35.7	17.1	29.3	10.5	29.4	23.6	28.5
	19.7	*35.0*	*32.2*	*39.5*	*16.9*	*34.1*	*7.9*	*29.4*	*25.7*	*34.7*
CO	**21.2**	**40.0**	**26.3**	**41.6**	**19.9**	**32.9**	**17.7**	**39.9**	**25.8**	**44.4**
	20.9	34.0	27.1	37.8	20.1	32.1	13.5	26.6	28.4	38.1
	21.1	*42.1*	*27.5*	*44.8*	*19.9*	*38.1*	*10.4*	*26.5*	*26.6*	*47.2*
CN	**20.0**	**44.1**	**22.9**	**44.9**	**16.4**	**36.1**	**15.1**	**34.8**	**26.8**	**42.7**
	20.0	36.5	25.7	45.6	16.6	31.7	11.5	29.1	26.8	36.4
	20.2	*44.4*	*31.8*	*49.8*	*18.0*	*40.3*	*8.5*	*32.7*	*28.5*	*46.0*
NH_3	**19.0**	**25.5**	**27.7**	**33.4**	**20.4**	**26.4**	**16.0**	**26.8**	**28.6**	**32.8**
	15.0	30.1	23.6	39.4	15.1	33.5	3.4	31.1	25.2	39.5
	16.7	*24.7*	*22.6*	*33.8*	*14.3*	*30.4*	*2.8*	*20.1*	*25.5*	*48.6*
CH_3	**15.3**	**32.3**	**18.8**	**35.0**	**11.7**	**24.4**	**10.8**	**28.3**	**20.8**	**31.3**
	16.2	25.4	22.8	32.1	13.4	23.7	7.0	23.1	20.5	26.2
	16.7	*33.8*	*29.2*	*40.8*	*14.6*	*30.9*	*4.6*	*25.1*	*22.6*	*35.9*
OH	**21.1**	**37.9**	**31.4**	**42.3**	**18.9**	**37.4**	**14.8**	**32.2**	**26.9**	**33.7**
	22.1	33.1	29.1	39.7	19.9	32.5	11.1	32.1	27.0	29.7
	22.0	*37.5*	*35.3*	*44.0*	*20.1*	*38.5*	*8.6*	*32.2*	*28.5*	*35.4*
H_2O	**19.9**	*b*	**29.1**	*b*	**23.3**	**24.5**	**11.8**	**22.2**	**26.7**	**28.7**
	16.5	34.0	24.1	38.7	16.8	37.5	3.7	29.0	24.3	39.3
	19.1	*22.8*	*30.6*	*29.4*	*13.4*	*20.8*	*2.1*	*18.2*	*23.6*	*46.4*

[a] Ti and Cr values are given in bold font; Zr and Mo values are in normal font, and Hf and W values are in italic font. [b] Broken structure.

and M−Z bonds. Also, thiametallatranes compute the least positive charge at the metal center which is due to extensive charge transfer from the three equatorial sulfur atoms to the central metal atom.

The stability of Group 6 metallatranes is higher than those of their Group 4 analogs, owing to the presence of stronger transannular M···N bonds in the former. The stability trend obtained for the aza derivative of these metallatranes is similar to those found for Group 4 analogs; i.e., the stability increases from NH to NCH_3 and decreases with $NSiH_3$. Like thiametallatranes of Group 4 elements, Group 6 ones are also strikingly more stable than oxametallatranes for the same reason as given for Group 4 analogs.

4. QTAIM Analysis

The topology of electron density in a molecule can be analyzed using Bader's atoms in molecules theory (AIM).[20] Generally, for covalent interactions (also referred to as "open-shell" or "sharing" interactions), the electron density at the bond critical point (BCP), ρ_b, is large (>0.2 a.u) while its laplacian, $\nabla^2\rho$, is large and negative. On the other hand, for closed-shell interactions (e.g., ionic, van der Waals, or hydrogen bonds), ρ_b is small (<0.10 a.u) and $\nabla^2\rho$ is positive. However, analysis of the bonding situation in transition metal compounds with QTAIM does not follow this usual notion since a covalent bond in transition metal compounds is characterized by a small value of ρ_b and small and positive values of $\nabla^2\rho$ due to the diffuse character of the electron distribution.[24] Hence, the bonding situation in these compounds cannot be described with ρ_b and $\nabla^2\rho$ alone, rather a more specific descriptor should be applied and electronic energy density $H(r)$ at BCP best fits the purpose.

Cremer and Kraka[25] proposed that a value of $H(r) < 0$ at BCP indicates the presence of significant covalent character and accounts for the lowering of potential energy of electrons at BCPs. The magnitude of $H(r)$ reflects the "covalence" of interaction. We have adopted a similar approach to characterize the transannular M···N bonds in Group 4 and 6 metallatranes (Tables S7 and S8, Supporting Information).[24−27] All these Group 4 metallatranes show a (3, −1) bond critical point at the M···N bond. The formation of (3, +1) ring critical points also support the presence of the transannular interaction which indicates the formation of five-member cycles in these molecules. As defined by Bader, the laplacian of electron density at BCP is give by $L(r) = \nabla^2\rho(r)$.[20a] The accumulation of electron density, ρ_b and a larger value of $L(r)$ along the bond path has an impact on the stability.[28a] Larger values of $L(r)$ and ρ_b result in local stabilization of the structure due to increased shielding of the nuclei of the bonded pair.[28b] Figure 2 shows a nice linear relationship between the transannular Ti···N distances with the electron density at the bond critical point, ρ_b, and its laplacian, $\nabla^2\rho$. Hence, stronger bonds are associated with larger accumulation of ρ_b and a larger value of $L(r)$. The laplacian at the bond critical point, $\nabla^2\rho$, are all positive and increase with a decrease in transannular M···N bonds. This is in tune with previous theoretical studies.[29−31]

The contour plot of laplacian (Figure 3) in the N···Ti−Z plane clearly shows the effect of apical as well as equatorial

(24) Farrugia, L. J.; Evans, C.; Tegel, M. *J. Phys. Chem. A* **2006**, *110*, 7952–7961.

(25) Cremer, D.; Kraka, E. *Angew. Chem., Int. Ed. Engl.* **1984**, *23*, 627–628.

(26) Macchi, P.; Sironi, A. *Coord. Chem. Rev.* **2003**, *238 − 239*, 383–412.

(27) Nakanishi, W.; Hayashi, S.; Narahara, K. *J. Phys. Chem. A* **2009**, *113*, 10050–10057.

(28) (a) Gatti, C. *Z. Kristallogr.* **2005**, *220*, 399–457. (b) Gibbs, G. V.; Downs, R. T.; Cox, D. F.; Ross, N. L.; Boisen, M. B., Jr.; Rosso, K. M. *J. Phys. Chem. A* **2008**, *112*, 3693–3699.

(29) Love, I. *J. Phys. Chem. A* **2009**, *113*, 2640–2646.

(30) Boily, J. *J. Phys. Chem. A* **2003**, *107*, 4276–4285.

(31) Henn, J.; Ilge, D.; Leusser, D.; Stalke, D.; Engels, B. *J. Phys. Chem. A* **2004**, *108*, 9442–9452.

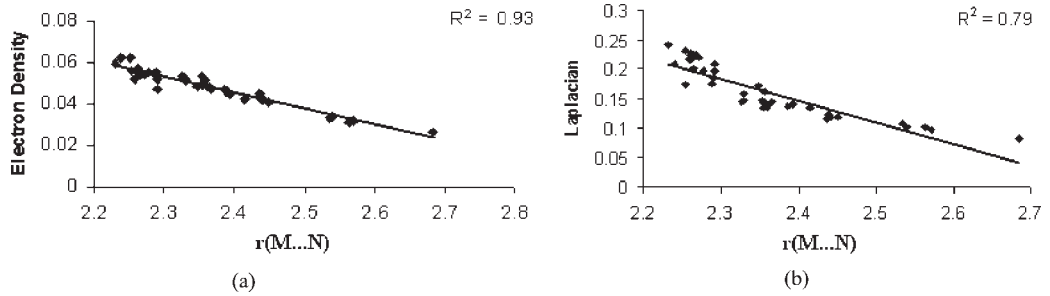

Figure 2. Variation of $r(M\cdots N)$ (Å) with (a) electron density (ρ, au) and (b) laplacian [$\nabla^2\rho$ (bcp), au] at the bond critical point of the transannular Ti···N bonds.

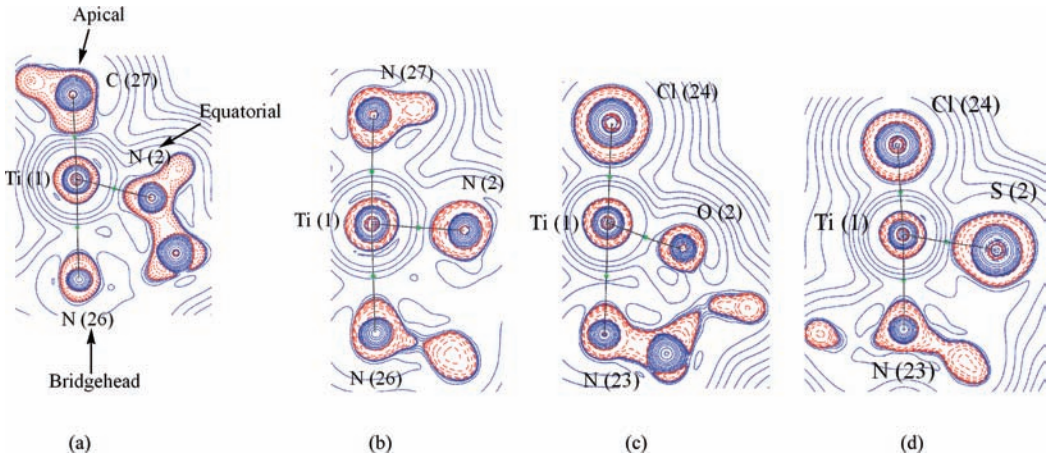

Figure 3. Contour plots of laplacian, $\nabla^2\rho$ (bcp), in the N···Ti−Z plane (obtained with AIMALL program[21] at B3LYP/6-31+G* level of theory) showing the effect of apical, (a) Z = CH_3 and (b) Z = NH_3, and equatorial substituents, (c) E = O and (d) E = S, on the bonding of titanatranes. Regions of charge depletion ($\nabla^2\rho > 0$) are denoted by solid blue lines while regions of charge concentration ($\nabla^2\rho < 0$) are denoted by dashed red lines. Green spheres denote bond critical points (BCPs), and black solid lines denote bond paths.

ligands in titanatranes. A clear distinction between the transannular interaction involving the two apical ligands, viz., CH_3 and NH_3, can be seen in Figure 3a,b which reflects a stronger transannular Ti···N interaction with NH_3 than CH_3, as the VSCC (valence shell charge concentration) on the bridgehead nitrogen atom is more polarized toward the titanium atom in the former. Figure 3c,d shows the effect of equatorial substituents on the M−E bond strengths. Charge transfer from equatorial substituent to the titanium atom is stronger with sulfur than oxygen which accounts for the stronger Ti−S bond strengths compared to Ti−O bonds.

The topological descriptions of electron density at the M···N (M = Zr, Hf) bond critical point is almost similar to those observed for Ti···N bonds (Table S7 and Figures S2 and S3, Supporting Information). The values of local electron density $H(r)$ are least negative for Zr···N bonds compared to other Group 4 metallatranes.

The topological values of the electron density at the transannular M···N bonds for Group 6 metallatranes are almost similar to that of Group 4 metallatranes (Table S8 and Figure S4, Supporting Information). However, there are some major contrasts in the topological character of Group 4 and 6 metallatranes. For example, Group 6 metallatranes compute higher values of ρ_b and $L(r)$ and more negative values of $H(r)$ at the M···N bond critical point compared to Group 4 metallatranes. All these topological parameters point toward a stronger transannular interaction in Group 6 metallatranes compared to Group 4 analogs. This is also reflected in the WBI values, stabilization energies, and delocalization index, δ(M, N), for the transannular M···N bonds of group 6 metallatranes(Tables S9 and S10, Supporting Information). Topological description of the M···N (M = Mo or W) bonds is quite similar to that of Cr···N bonds (Figure S5 and S6, Supporting Information).

The distribution of laplacian at the Cr···N bond critical points is shown in Figure 4 which illustrates the effect of apical as well as equatorial substituents on the Cr···N and Cr−E bond strengths. As seen for titanatranes, similar, but somewhat more, polarization of the VSCC on bridgehead nitrogen toward chromium is noticed here.

Thus, the M···N bond critical point shows low values of ρ_b, small and positive values of $\nabla^2\rho$, and negative values of $H(r)$. All these computed topological descriptors at the transannular M···N bond critical points of Group 4 and 6 metallatranes show a considerable degree of covalency which increases from Group 4 to Group 6. Stronger transannular bonds have higher values of delocalization index δ(M, N; Figure S7, Supporting Information), electron density, ρ_b, and higher values of $L(r)$. The calculated Ehrenfest forces[32] for the metal atom are attractive in every case drawing the metal atom toward the bridgehead nitrogen atom. This attractive Ehrenfest force results in a stabilizing energy for the formation of $M|N_b$ (N_b is the bridgehead atom) surface. The external contribution to the nuclear−electron potential energy at the metal center $\Delta V^e ne(M)$ dominates over the own contribution $\Delta V^0 ne(M)$, which accounts for the stability of these molecules (Tables S9 and S10, Supporting Information).

(32) Ehrenfest, P. *Z. Phys.* **1927**, *45*, 455.

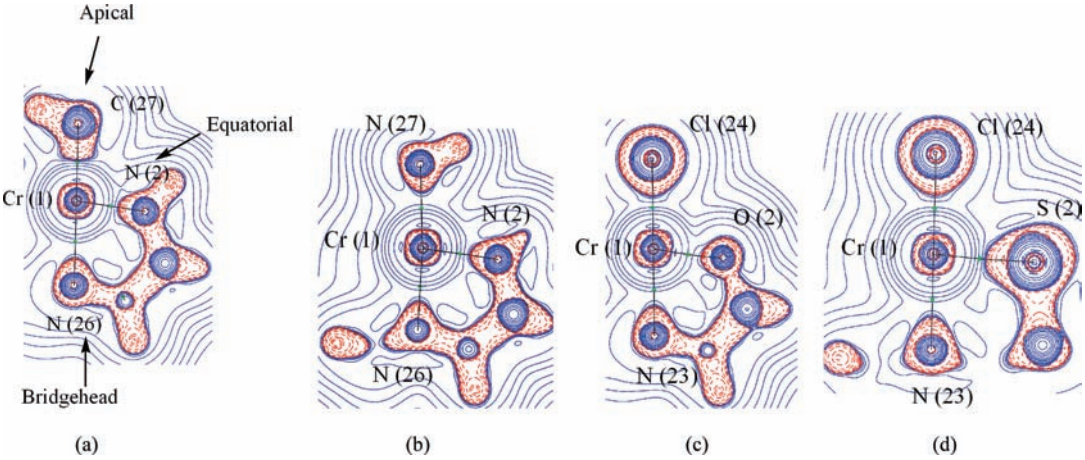

Figure 4. Contour plots of laplacian, $\nabla^2\rho$ (bcp), in the N···Cr−Z plane (obtained with AIMALL program[21] at B3LYP/6-31+G* level of theory) showing the effect of apical, (a) Z = CH_3 and (b) Z = NH_3, and equatorial substituents (c) E = O and (d) E = S, on the bonding of chromatranes. Regions of charge depletion ($\nabla^2\rho > 0$) are denoted by solid blue lines while regions of charge concentration ($\nabla^2\rho < 0$) are denoted by dashed red lines. Green spheres denote bond critical points (BCPs), and black solid lines denote bond paths.

5. Conclusions

The nature of intramolecular transannular M···N bond, a key structural feature of Group 4 and 6 metallatranes, are found to be influenced not only by the substituents at apical and equatorial positions but also by the extent to which the metal and bridgehead nitrogen atoms are pyramidalized. Shorter and stronger M···N bonds are computed for molecules in which the metal atom is slightly pyramidalized whereas the bridgehead nitrogen atom is strongly pyramidalized. Weakly trans directing apical ligands such as Cl, NH_3, and H_2O strengthen the transannular interaction while the stronger ones CO, CN, and CH_3 weaken the same. The M···N bonds of Group 6 metallatranes are found to be stronger than their Group 4 analogs, and accordingly, higher stabilization energies are computed for the former. The energetics of different spin states of Group 6 metallatranes are found to depend on the nature of apical as well as equatorial substituents. The nature of the transannular bond of these molecules was ascertained with the help of QTAIM analysis which reveal that they have (i) small values of electron density (ρ_b), (ii) small and positive values of laplacian ($\nabla^2\rho$), and (iii) negative values of local electronic energy density [$H(r)$] at the bond critical points. Thus, the M···N bonds of these molecules have a considerable amount of covalent character.[26] Ehrenfest forces for the metal atom are all attractive in nature, and the atomic contribution for the stability of these molecules comes from large negative values of external contribution to nuclear−electron potential energy at the metal center, $\Delta V^e ne$. We feel that our study will further help the experimentalists in designing new and efficient metallatrane based catalytic systems.

Acknowledgment. A. K. P. thanks the Department of Science and Technology (DST), New Delhi for providing financial assistance in the form of a project (project no. DST/FTP/CS-85/2005). A. K. G. thanks Tezpur University for institutional fellowship. We thank one of the reviewers for inspiring us to make a more critical and deeper analysis of the results obtained from QTAIM calculation which ultimately helped us in improving the manuscript.

Supporting Information Available: Tables S1−S10 and Figures S1−S7, complete reference for Gaussian 03 (reference 19), and the Cartesian coordinates of the optimized geometries of all the Group 4 and 6 metallatranes. This material is available free of charge via the Internet at http://pubs.acs.org.